Visualization of sound waves using regularly spaced soap films

F Elias[1], S Hutzler[2] and M S Ferreira[2]

[1] Laboratoire Matière et Systèmes Complexes, Université Paris 7 and CNRS UMR 7057,
Batiment Condorcet, case 7056, 10 rue Alice Domon et Léonie Duquet, 75 205 Paris Cedex 13,
France
[2] School of Physics, Trinity College, Dublin 2, Republic of Ireland

E-mail: elias@ccr.jussieu.fr

Abstract
We describe a novel demonstration experiment for the visualization and
measurement of standing sound waves in a tube. The tube is filled with
equally spaced soap films whose thickness varies in response to the amplitude
of the sound wave. The thickness variations are made visible based on optical
interference. The distance between two antinodes is easily measured using a
ruler and the determined wavelengths of the modes of the standing wave are in
excellent agreement with the theory.

(Some figures in this article are in colour only in the electronic version)

1. Introduction

Soap films and bubbles have been used for teaching elementary physics and geometry for
over a century. Many demonstrations by Boys [1], first published in 1890, are still in the
standard bag of tricks of lecturers in these fields (a careful reading of the book might lead to a
rediscovery of many others). Recent collections of old and new experiments can be found in
the books by Rämme [2, 3].

Bubbles are easy to produce, but their shapes and colours are intriguing and fascinate old
and young audiences, independent of their scientific background. Their use in teaching is also
advantageous as they make the experiments cheap, safe and environmentally friendly.

Traditionally, experiments cover physical properties of thin films, such as interference
colours, or surface tension related phenomena. However, soap films are also useful as
analogies to other physical systems or topics in mathematics, such as atomic models [2],
catastrophe theory [4] or minimization problems [5].

In this paper we describe experiments where soap films are used to both visualize sound
waves and determine their propagation velocity. The films act as vibrating membranes whose
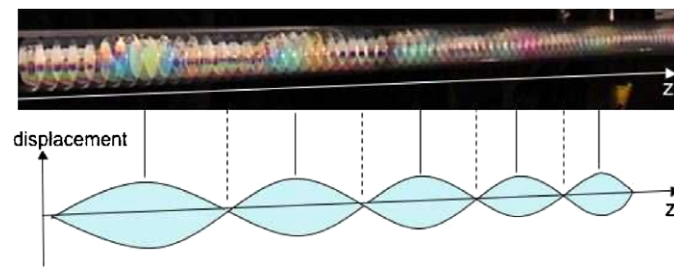
Figure 1. A standing sound wave in a perspex tube may be visualized by the presence of equally spaced soap films. Coloured soap films reveal the antinodes. The sketch shows the amplitude of the fluid displacement corresponding to the standing wave (note that both photograph and sketch display a certain angle of observation).

vibrations lead to a redistribution of the liquid they contain. This is made visible by optical interference.

Whereas many teaching demonstrations show transversal waves (i.e. waves on a string or waves at the surface of water), only very few experiments allow for the visualization of longitudinal waves. The technique proposed below is an alternative to the so-called Kundt tube experiment in which a standing acoustic wave is visualized by the displacement of a light powder [6]. In our set-up, equally-spaced soap films are placed inside a cylindrical perspex tube. The films are oriented perpendicularly to the tube axis. The effect of a standing acoustic wave is that the soap films which are situated near the displacement *antinodes* vibrate and swell, whereas those close to the displacement *nodes* remain thin and static. This is readily made visible by directing a light source towards the tube. The photograph of figure 1 shows the visualization of the standing wave based on optical interference.

The experiments presented in this paper are based on two facts: first, the soap film thickness is a function of the local amplitude of the sound wave; second, the soap film thickness is visible optically. In the following, we present the background on the physics of soap films and their observation using white light interference. We also recall the principle of acoustic resonance in an empty tube. We then present the experimental set-up and procedure, first for the production of equally spaced soap films in the tube, secondly for the generation and analysis of an acoustic standing wave, and finally, for the visualization of the vibration of the soap films. We show that this technique indeed captures the resonances of the tube and that we can accurately measure the corresponding wavelengths. We conclude by briefly discussing the relevance of acoustic standing waves for current foam research.

2. Background

2.1. Thickness of a soap film

A soap film is a thin layer of liquid. It is made of an aqueous soap solution confined between two interfaces, which are stabilized by the adsorption of surfactant molecules [5]. A soap film is usually created by pulling a frame out of a soap solution, or by blowing air through the solution. Because of the pressure differences within the film (capillary pressure or hydrostatic pressure), its thickness depends on time, and goes from 10 μm when the film is created to a few nanometres at equilibrium [5]. The equilibrium thickness of the film is reached when the interfaces are close enough to interact: the interaction, either electrostatic or steric, is

repulsive, and therefore prevents the soap film from thinning. In a vertical soap film, the film thickness depends on the height because of gravity: since the liquid solution falls downwards within a film until equilibrium is reached between gravity and capillarity, the soap film is thicker at the bottom and thinner at the top.

2.2. Colours of a soap film

When the soap film thickness is comparable to the wavelength of light, the light beam reflected (respectively transmitted) by the two interfaces of the film interfere. Therefore, the intensity of light reflected (respectively transmitted) by the soap film depends on the soap film thickness. Let us consider a soap film illuminated with a monochromatic light (wavelength in air λ_{light}) at an incident angle θ. The light intensity I reflected by the soap film is given by [5]:

$$I(\lambda_{\text{light}}) = 2RI_0 \left[1 + \cos\left(\frac{2\pi\delta}{\lambda_{\text{light}}}\right) \right] \qquad \text{with} \qquad \delta = 2t\sqrt{v^2 - \sin^2\theta} + \lambda_{\text{light}}/2. \qquad (1)$$

Here R is the reflectivity of light at the interface of the soap film, I_0 is the intensity of the incident light, δ is the difference in path length of the two beams, t is the soap film thickness and v is the refractive index of the soap solution (the typical values found in the literature for different aqueous soap solutions are $v \sim 1.4$ to 1.5 in the visible range). The second term of half a wavelength in the expression of δ is due to the fact that one of the interfering beams is reflected at an optically thick medium (from air to the soap solution), whereas the second beam is reflected at an optically thin medium (from the soap solution to the air). According to the Fresnel equations, this second reflection adds a phase shift of π to the expression of the reflected light wave, which leads to the additional term $\lambda_{\text{light}}/2$ in equation (1).

If the film is illuminated with a white light, composed of all colours of the visible spectrum, each wavelength has an emerging intensity given by equation (1). The intensity and spectral composition of the emerging beam results from the sum of the contributions from each wavelength. As for each wavelength the light intensity is a (periodic) function of the film thickness t this results in a colouring of the films according to their thickness. For $\delta \simeq \langle\lambda_{\text{light}}\rangle \simeq 600$ nm (corresponding to $t \simeq 100$ nm if $\theta = 45°$), the intensity of the reflected light is close to its maximum for all the wavelengths of the visible range. A silvery white fringe is then observed. For $\delta > 600$ nm, the succession of colours appears as a periodic function of the film thickness (Newton colours). It is indeed possible to identify individual colours with corresponding film thickness in the range 100–1500 nm [5].

For film thicknesses smaller than the wavelengths of visible light the optical path difference δ in equation (1) is essentially due to the phase shift for reflection at the air–solution interface, as mentioned above. Setting $\delta = \lambda_{\text{light}}/2$ results in zero intensity for reflection. In practice, films with thickness smaller than about 30 nm are transparent; therefore they appear black if a black screen is placed behind the film. The thinnest soap films (Newton black films) have a thickness of about 5 nm [5].

Figure 2 shows an image of vertical soap films in the tube used in the experiments (in the absence of sound waves). As a result of gravity-driven drainage the vertical films are thinner at the top and thicker at the bottom. The top of the films are black. The middle part of the films, silvery white in appearance, have a nearly homogeneous thickness of the order of $t \sim 100$ nm. At the bottom of the films, thin coloured horizontal stripes are observed which clearly indicate the vertical thickness gradient. At the very bottom the films are transparent because the optical path length is larger than the coherence length of the light; therefore the reflected beams do not interfere. The transparent film appears black if a black screen is placed behind the film.
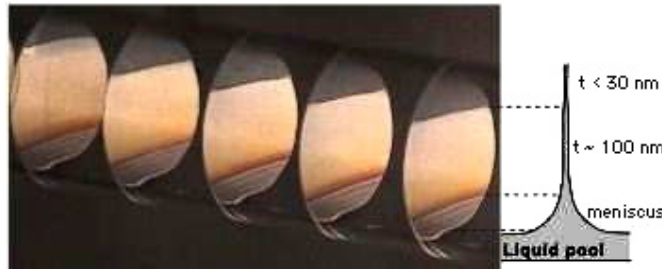
Figure 2. Interference pattern observed using the setup of figure 5 in the absence of sound waves. The soap films are vertical and display a variation in colour (thickness) due to the gravitationally driven drainage. The sketch at the right of the figure shows a cross-section of the film. *t* is the film thickness. The film has reached its equilibrium thickness only in the top region (black film), and is still draining in the white and the coloured regions.

2.3. Acoustic resonances of a tube

Let us consider a tube of length L filled with air at ambient temperature and pressure. The tube is closed at both ends, and an acoustic wave of wavelength λ is present in the tube. The incident propagative wave and the reflected wave in the tube add up, leading to a standing acoustic wave in the tube. Because of the boundary conditions (maximum amplitude at the open ends), only a discrete number of frequencies f_n are allowed for this standing wave:

$$f_n = n\frac{c}{2L}, \tag{2}$$

where n is an integer number called the *resonant mode*, and c is the sound velocity in air. The associated wavelength of the resonant mode n of the tube is then given by

$$\lambda_n = c/f_n = 2L/n. \tag{3}$$

Therefore, if the frequency of the incident acoustic wave is continuously increased keeping the amplitude constant, the intensity of the standing wave in the tube will be maximal only when $f = f_n$. At those frequencies, $n/2$ wavelengths are present in the tube.

2.4. Soap films in an acoustic wave

Under the effect of a compressive wave propagating in the surrounding air, soap films vibrate at the frequency of the excitation. Many observations and studies exist in the literature on the subject of soap film undulations (see [7–11] and references therein). Unlike the skin of a drum, soap films are not simple membranes. In response to acoustic waves the thickness of a film may change locally due to a redistribution of the liquid in the film [11]. Liquid may also be squeezed out of the film into a reservoir of liquid. Such effects are at the heart of many complicated and fascinating patterns observed in soap films in the presence of sound waves.

The main purpose here is not to study the details of these undulations but merely to make use of them for the detection of standing waves. This detection is based on the fact that the change of thickness of soap films in response to a sound wave is accompanied with a change in colour when the film is illuminated with white light, which makes this modification visible to the eye in a spectacular way. Section 3.4 shows images and a brief description of the vibrating soap films observed in our experiments.
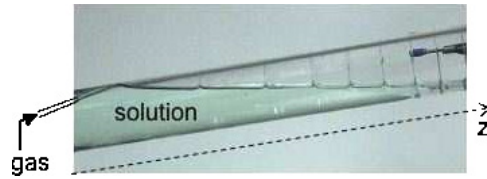
Figure 3. The gas is injected at a constant flow rate just below the surface of the solution in the tilted tube.

3. Experimental setup and procedure

3.1. Large bubble generation

The cylindrical perspex tube used in the experiment has an internal diameter $\phi = 35$ mm and a length $L = 2.05$ m. The large dimensions facilitate the observation of the films, and also increase the number of wave nodes/antinodes in the tube. The soap solution is made from tap water and surfactant solution (commercial dish-washing solution 'Fairy liquid' by Procter and Gamble) at a volume fraction of about 5%.

Monodisperse soap bubbles are usually formed by injecting gas at a constant flow rate through a nozzle immersed in surfactant solution. Confined in a cylindrical tube of internal diameter comparable to the bubble size, the bubbles arrange in a perfect periodical lattice, whose elementary cell depends on the ratio between the tube and the bubble diameter [12, 13]. The simplest structure, a single row of bubbles or 'bamboo structure' (corresponding to equally spaced soap films oriented perpendicular to the tube axis) is obtained if this ratio is less than approximately 1.1. For our tube diameter this requires bubble volumes larger than 30 cm^3.

In the limit of small gas flow rate, a bubble emerging from a nozzle of internal diameter d has a volume V whose value at detachment may be estimated by considering the equilibrium of forces acting on it. Equating the buoyancy force with the surface tension force that attaches the bubble to the nozzle one obtains [14]

$$V \sim \frac{\pi d \gamma}{\Delta \rho g}. \tag{4}$$

Here γ, $\Delta \rho$ and g are the surface tension, density difference of liquid and gas, and gravitational acceleration, respectively.

According to equation (4) creating equally spaced soap films in our wide tube requires a nozzle of internal diameter $d \sim 10$ cm, too large to be convenient for an experiment. An alternative to equation (4) would be to increase the bubble volume by increasing the gas flow rate through the nozzle. However the production of such large bubbles would require a large gas flow rate, leading to various instabilities that result in bubble polydispersity.

We therefore introduce a new technique, which easily produces large monodisperse bubbles. This is achieved by placing the nozzle close to the air/liquid interface in a nearly horizontal tilted tube, as shown in figure 3. A rubber stopper, in which the nozzle (internal diameter: 2 mm) is inserted, seals the lower end ($z = 0$) of the tube. The tube is then partly filled with soap solution and tilted towards the horizontal. The nozzle is adjusted so that its opening is just below the air/liquid interface, close to the tube wall. Gas is injected at a constant flow rate (~ 150 ml min^{-1}). As a bubble forms at the interface it slowly slides upwards along the tube walls. Since most of its volume is above the interface its buoyancy is reduced, which according to equation (4) leads to an increase of the bubble volume. After
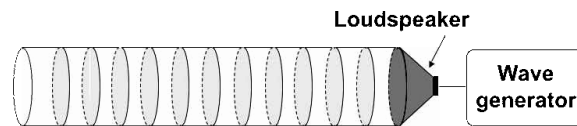
Figure 4. Production of a standing sound wave.

the tube has been filled with the bamboo structure, we carefully remove the stopper at the lower end in order to empty the excess of soap solution from the tube. We then place the tube horizontally.

We find that the bubble size obtained in this procedure is highly reproducible within a precision of 10% on the spacing between two consecutive soap films. The spacing mainly depends on the depth at which the nozzle tip is immersed in the solution and increases as we tilt the tube nearer towards the horizontal. Here, we used spacings between 1 cm and 2 cm.

There is a small systematic increase in bubble size for a given fixed tube as we fill the tube which can be understood as follows. Once a bubble is formed, it carries along a small but finite amount of liquid as it moves up the tube. This leads to a steady decrease in the amount of liquid surrounding the nozzle at $z = 0$. Therefore, the immersion depth of the nozzle decreases in time and the bubble size increases. Since our visualization of sound waves does not depend on the equal spacing of soap films, we have not suppressed this effect. If needed, this issue could be solved in principle by connecting the soap solution at the bottom of the tube to a reservoir.

We also note that there always remains a small amount of soap solution in the tube, which forms a shallow pool at the bottom of the horizontal tube, hence forming a liquid bridge between all the films. This serves as a reservoir of soap solution to the films, allowing them to adapt their thickness in the presence of a sound wave.

It takes approximately 4 min to fill the tube with the regularly spaced soap films. The experiment does not require the soap films to have reached their equilibrium thickness, and can start immediately after the tube has been placed horizontally.

3.2. Production of an acoustic standing wave in the tube

An acoustic wave is generated in the tube by attaching a loudspeaker at one end (at $z = 205$ cm) which is connected to a frequency generator in order to vary the wave frequency in the audio range 20–20 000 Hz. The other end of the tube ($z = 0$) is closed to air (figure 4). The analysis presented below requires no microphone nor oscilloscope, although they might be used for a quantitative comparison.

3.3. Visualization using white light interference

When the foam is subjected to an acoustic standing wave, the liquid in the films flows from the high-pressure region (displacement nodes) to the low-pressure region (displacement antinodes). As a result, the film thickness varies along the tube axis. Gradients of thickness within individual films can also appear in response to sound waves. Both these effects (figures 5, 6 and 7) can be observed by illuminating the tube with plane white light with an incident angle θ. An effective light source is provided by an ordinary overhead projector which provides a satisfactory plane illumination over the volume occupied by the tube.

The light reflected by the soap films is observed at the angle $-\theta$ using a digital camera. θ must be small enough to optimize the area of observation, but large enough to resolve
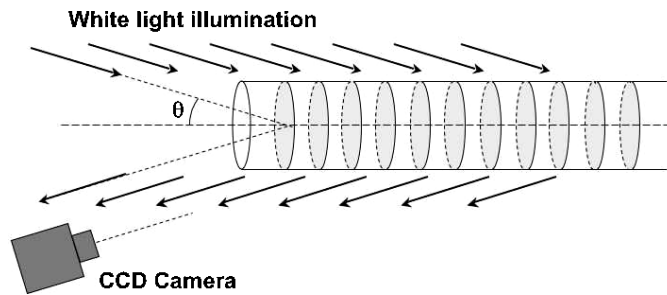
Figure 5. Visualization of the film thickness gradients using white light interference.

Figure 6. Close-up of soap films subject to a standing sound wave. The central film is located at an antinode. The error on the relative position of the film with respect to the antinode is equal to the spacing between the films, that is 1 cm. The colour of a film corresponds to a certain film thickness which increases with the amplitude of the standing wave. Here the frequency of the sound wave was 670 Hz. According to equation (2), this corresponds to $n = 8$ with $c = 340$ m s^{-1}.

between different films. We chose $\theta = 45°$ and also placed a black screen behind the tube to increase the contrast of the images.

This set-up allows the observation, in a single image, of the interference patterns displayed by all the soap films in the tube.

3.4. Observation of soap film vibration

In response to an acoustic wave, soap films vibrate. Since the soap films are connected to a reservoir of solution at the bottom of the tube, the film thickness is a free variable. Using the set-up described in section 3.3, we observed that the soap films change colour when they vibrate. Figure 6 shows a close-up of five soap films centred around a displacement anti-node of the wave. The film in the centre (at the antinode) appears green, its neighbouring films appear blue and the next-nearest neighbours are brownish. This symmetry in colours around the central film mirrors the symmetry of the displacement amplitude of the sound wave around an antinode. The larger the wave amplitude, the thicker the soap film.

Figure 6 shows an additional interesting phenomenon. The soap films display a stationary radial undulation pattern. The vibration of the film in response to the acoustic resonance of the tube is limited by the boundary condition at the perimeter of the film, where the longitudinal displacement of the film must vanish. Therefore, the soap film experiences a standing vibrational wave as a result of the superposition of an incident and a reflected propagating wave.
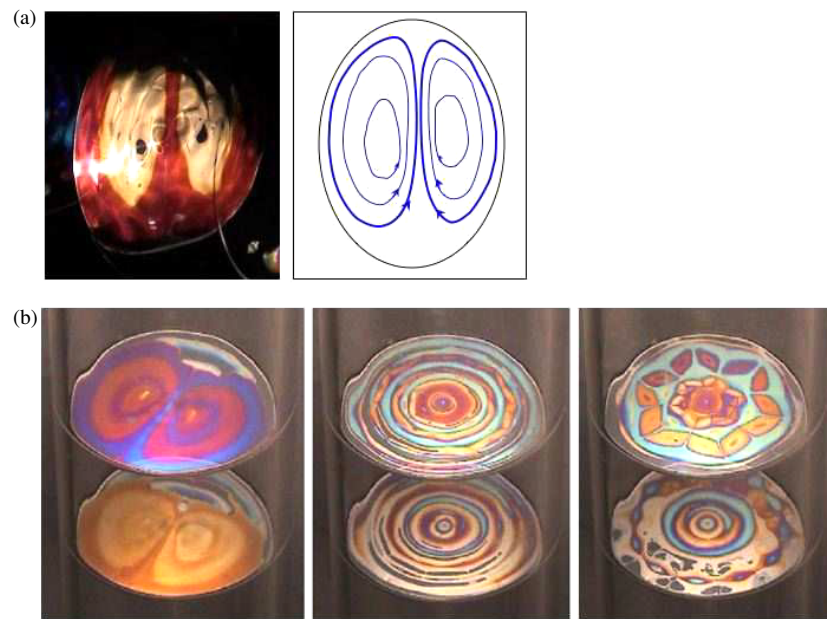
Figure 7. For sound frequencies above 850 Hz vibrating soap films display vibration patterns due to occurring thickness gradients. (a) *Vertical* soap films at 850 Hz, together with a sketch of the observed flow of the interstitial liquid. (b) *Horizontal* soap films. The photos are taken at different resonant frequencies of the tube (all exceeding 850 Hz).

Soap films display two possible kinds of behaviour in response to a sound wave [9, 10]. At low excitation frequencies, the soap film interfaces vibrate in phase with the same amplitude (*antisymmetric mode*, or *undulation mode*), therefore their thickness remains homogeneous. At high excitation frequency, thickness gradients are observed, resulting in complex and beautiful patterns, sometimes coupled to a flow of interstitial fluid. We observe those two regimes with a transition frequency of 850 Hz. Figure 6 corresponds to the first regime (homogeneous thickness). Figure 7 shows examples of soap films vibrating in the second regime. In figure 7(a), two counter-rotative vortices in a vertically oriented film reveal a decrease in thickness towards the centre of the vortices. In the photographs of figure 7(b) the soap films in the tube have been placed horizontally in order to observe more patterns on soap films in a radial symmetry (the tube is vertical). The three images correspond to different frequencies above 850 Hz. The image on the left shows counter-rotative vortices similar to figure 7(a). The image in the centre has a radial symmetry. The image on the right shows a more complex pattern, with a six-fold symmetry. For the same excitation frequency, the particular pattern adopted depends on the initial film thickness and on the amplitude of the vibration. This can be seen from the image on the right of figure 7(b), where two films vibrating at the same frequency but at different amplitudes display different patterns. Similar observations for individual soap films were presented by Sedley Taylor in 1878 [7]. His publication is appended by 14 careful drawings of vibration patterns of soap films in circular, square and triangular confinement.

In the horizontal tube as in the vertical tube, the motion of fluid within the soap film is observed as soon as an acoustic wave is present in the tube. However, it takes a few minutes for the patterns to stabilize (figures 6 and 7), since the liquid has to redistribute within a very thin soap film.
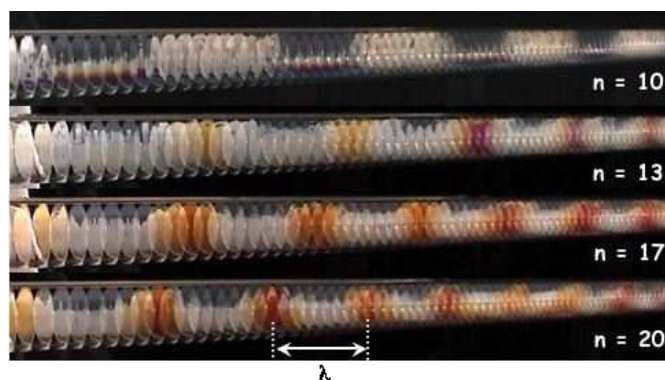
Figure 8. Photographs showing the tube filled with soap films in the presence of standing sound waves for different resonant modes n of the tube. The thicker coloured films are placed at the antinodes. The wavelength corresponds to the distance between the coloured films.

### 3.5. Detection of standing waves along the tube

The presence of an acoustic standing wave along the tube leads to an adaptation of the thickness of a soap film to the local amplitude of the wave. Therefore, the vibrations of the soap films make the tube resonances visible to the eye. The resonances can then be detected visually, without the help of a microphone and an oscilloscope, in the following way: in the range of the audio frequencies emitted by the loudspeaker, we slowly and continuously increase the frequency. At each resonance of the tube the soap films at or close to the anti-nodes vibrate with a strong amplitude. Figure 8 shows images of the soap films in the tube when the imposed frequency matches a resonant frequency of the tube. At the antinodes of the standing wave, the soap films vibrate and change colour. This experiment makes the resonance phenomenon spectacular, and clearly exhibits the discrete nature of the number of resonance modes.

3.5.1. Counting the resonant modes. We have counted the tube resonant frequencies, detected in such a way. The results are plotted in figure 9, where Δn is a counting index ($\Delta n = 1$ for the first resonance that is visually detected when the excitation frequency is slowly increased from zero).

The data may be compared to the theory presented in section 2.3. Since the loudspeaker is placed at one end of the tube, the displacement amplitude is maximum and the resonant modes are the same as those with the tube closed at both ends. The frequency f_n of the resonant mode n of the tube is therefore given by equation (2).

In the method described here, all the measured successive resonant frequencies of the tube are labelled without knowledge of the mode number of the first resonant mode that we detect. In figure 9 we therefore plot f_n versus our counting index $\Delta n = n - n_0$, where n_0 is the first detected resonant mode (or offset). We find that the frequency increases linearly, the initial resonant mode n_0 is determined by a least-squares fit using equation (2), with $n = \Delta n + n_0$.

3.5.2. Wavelength measurement. The wavelength of the standing sound wave can be determined directly on the tube wall, by measuring with a ruler the distance between displacement antinodes, made visible by the soap film vibration (see figure 10). The error bar then corresponds to the distance between two soap films, and could in principle be decreased
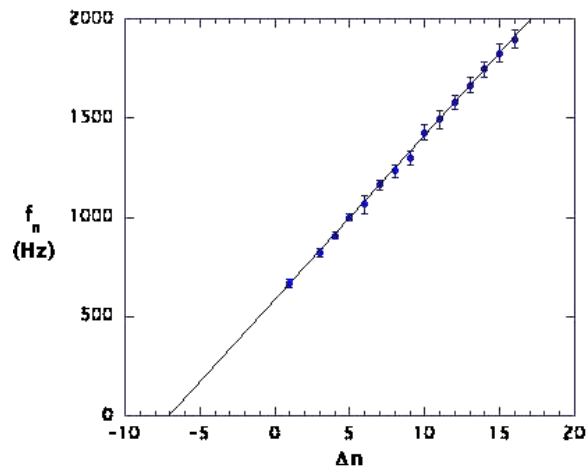
Figure 9. Resonant frequency as a function of the counting index (mode number) $\Delta n = n - n_0$, counted from the initial visible resonant mode n_0. The solid line represents a fit of the data using equation (2) where n is replaced by $\Delta n + n_0$ and n_0 is the only fitting parameter. One finds $n_0 = 7$.
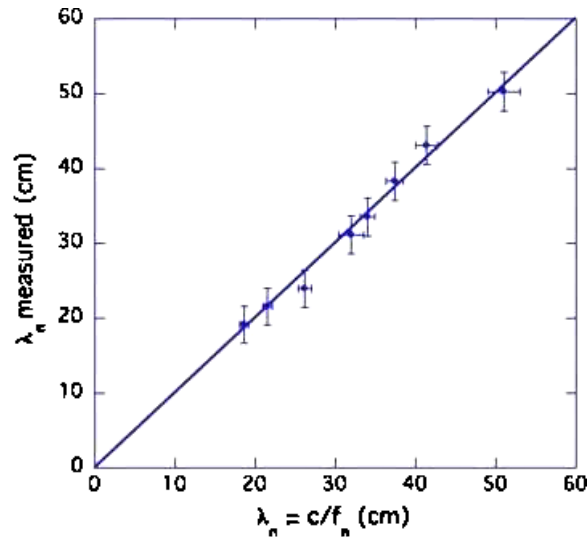
Figure 10. Measured wavelengths for different resonant modes ($n = 8, 9, 10, 12, 13, 16, 19$ and 23) plotted against the theoretical values given by equation (3). The straight line has slope one.

if the film spacing is decreased. With our previous determination of n_0 and using equation (2) we can compare these values directly with the values given by equation (3).

Figure 10 shows a plot of the experimentally determined values for λ_n versus the values computed using equation (2) where we used the value of sound in air for c ($c = 340$ m s^{-1} at 20 °C). The data points are well described by a straight line of slope one, passing through the origin, and thus verifying the validity of our technique.

Let us note that the presence of a foam usually decreases the sound velocity: the wetter the foam the lower the sound speed [15]. However in the case studied in this paper, the

amount of liquid in the soap films is small enough for the sound velocity not to be affected by the presence of the foam. Using an oscilloscope we verified that the measured resonance frequencies of the empty tube are the same as the resonance frequencies of the tube filled with soap films.

4. Conclusion

We have presented a simple experiment that allows the visualization of sound waves in a cylindrical tube using homogeneously spaced soap films. Antinodes are easily detectable by the visible thickening of the films in their vicinity. The spacing between antinodes, measured with a ruler, gives (half) the wavelength of standing sound waves in the tube. Variation of the sound frequency allows for the identification of modes.

Following in the tradition of a long list of experiments that employ soap films and bubbles in teaching physics, this experiment is cheap, reliable and easy to perform in classroom demonstrations. It might also lend itself to student experiments, possibly in addition to experiments exploring effects of surface tension. Furthermore, a discussion of interference effects, in particular in relation to the thickness of black films, might even lead to presenting soap films as very tangible objects in the realm of fashionable nano-science.

Acknowledgments

References

[1] Boys C V 1890 *Soap Bubbles and the Forces which Mould Them* (London: SPCK)
   Boys C V 1959 *Soap Bubbles, their Colours and the Forces which Mould Them* (New York: Dover) (enlarged edition)
[2] Rämme G 1998 *Soap Bubbles in Art and Education* (Singapore: Willie Yong)
[3] Rämme G 2006 *Experiments with Soap Bubbles and Soap Films* (Rämme: Uppsala, Sweden)
[4] Lovett D R 1994 *Demonstrating Science with Soap Films* (Bristol and Philadelphia: Institute of Physics Publishing)
[5] Isenberg C 1987 *The Science of Soap Films and Soap Bubbles* (Clevedon, Avon, UK: Tieto)
   Isenberg C 1992 *The Science of Soap Films and Soap Bubbles* (New York: Dover) (reprinted)
[6] A demonstration movie can be seen at the following address: http://hyperphysics.phy-astr.gsu.edu/hbase/waves/kundtosc.html
[7] Taylor S 1878 *Proc. R. Soc.* **27** 71
[8] Dewar J 1923 *Proc. R. Inst.* **24** 197
[9] Couder Y, Chomaz J M and Rabaud M 1989 *Physica* D **37** 384
[10] Taylor G I 1959 *Proc. R. Soc.* A **253** 296
[11] Boudaoud A, Couder Y and Ben Amar M 1999 *Phys. Rev. Lett.* **82** 3847
[12] Hutzler S, Weaire D, Elias F and Janiaud E 2002 *Phil. Mag. Lett.* **82** 297
[13] Weaire D and Hutzler S 1999 *The Physics of Foams* (Oxford: Oxford University Press)
[14] Drenckhan W, Elias F, Hutzler S, Weaire D, Janiaud E and Bacri J-C 2003 *J. Appl. Phys.* **93** 10078
[15] Gardiner B S, Dlugogorski B Z and Jameson G J 1998 *J. Rheol.* **46** 1437